ADVANCES IN ATMOSPHERIC SCIENCES, VOL. 28, NO. 6, 2011, 1279–1290

Effect of Stochastic MJO Forcing on ENSO Predictability

PENG Yuehua[1,2,3] (彭跃华), DUAN Wansuo*[1] (段晚锁), and XIANG Jie[3] (项 杰)

[1] *The State Key Laboratory of Numerical Modeling for Atmospheric Sciences and Geophysical Fluid Dynamics, Institute of Atmospheric Physics, Chinese Academy of Sciences, Beijing* 100029

[2] *Department of Military Oceanography, Dalian Naval Academy, Dalian* 116018

[3] *Institute of Meteorology, PLA University of Science and Technology, Nanjing* 211101

(Received 13 January 2011; revised 1 April 2011)

ABSTRACT

Within the frame of the Zebiak-Cane model, the impact of the uncertainties of the Madden–Julian Oscillation (MJO) on ENSO predictability was studied using a parameterized stochastic representation of intraseasonal forcing. The results show that the uncertainties of MJO have little effect on the maximum prediction error for ENSO events caused by conditional nonlinear optimal perturbation (CNOP); compared to CNOP-type initial error, the model error caused by the uncertainties of MJO led to a smaller prediction uncertainty of ENSO, and its influence over the ENSO predictability was not significant. This result suggests that the initial error might be the main error source that produces uncertainty in ENSO prediction, which could provide a theoretical foundation for the data assimilation of the ENSO forecast.

Key words: Madden–Julian Oscillation (MJO), El Niño–Southern Oscillation (ENSO), conditional nonlinear optimal perturbation (CNOP), model error

Citation: Peng, Y. H., W. S. Duan, and J. Xiang, 2011: Effect of stochastic MJO forcing on ENSO predictability. *Adv. Atmos. Sci.*, **28**(6), 1279–1290, doi: 10.1007/s00376-011-0126-4.

1. Introduction

ENSO is the most prominent interannual signal in the climate system and has large effects on the global climate. Knowledge about the ENSO cycle and the ability to forecast its variations can provide valuable information to professionals in the fields of agriculture, public health and safety, fisheries, forestry, and many others in climate-sensitive professions (Huang, 1999; Zhang et al., 2003). Therefore, simulation and prediction of the ENSO is very important.

ENSO is by far the most predictable short-term fluctuation in the Earth's climate system (Chen and Cane, 2007). However, considerable uncertainty remains in ENSO predictions (Tang et al., 2008; Luo et al., 2008). Many studies have been conducted on the ENSO predictability method regarding initial error growth. Moore and Kleeman (1996) investigated the spring predictability barrier (SPB) and revealed the impact of the initial error on ENSO predictability. Xue et al. (1997) also demonstrated that the ENSO prediction level was dependent on the initial field precision of the numerical model. Chen et al. (1995, 2004) reduced the SPB and enhanced the ENSO prediction accuracy of the Zebiak-Cane model by improving the model initialization, among others. Recently, Mu et al. (2007a, b) and Duan et al. (2009b) further studied ENSO predictability and displayed the effect of the transient growth of initial errors caused by nonlinear instability, and their results showed that the initial errors with specific spatial structure can lead to significant SPBs. Duan et al. (2009b) and Yu et al. (2009) recognized two types of initial errors using statistical and dynamical methods, respectively; they demonstrated that the dynamical mechanisms of error growth were related to the SPB.

The aforementioned studies primarily investigated the effect of initial errors on ENSO predictability. In general, the uncertainty of climate prediction is caused by initial error and model error. The effect of model error on ENSO predictability can be meaningful. Duan and Zhang (2010) studied the effects of initial error

*Corresponding author: DUAN Wansuo, duanws@lasg.iap.ac.cn

and model error caused by parameter uncertainty on ENSO predictability with a theoretical ENSO model. Compared with initial error, their results showed that the prediction error produced by parameter uncertainty was relatively small and did not have a significant impact on ENSO predictability. The uncertainty of the external forces was also an important source of model error. Then how do they affect ENSO predictability?

The Intraseasonal Oscillation or the Madden–Julian Oscillation (ISO/MJO) is considered to be one of the main external forces affecting ENSO, even though a great deal of dispute remains concerning their relationship. Some insist that MJO is one of the mechanisms that provoke El Niño events and that MJO has a significant effect on the ENSO (Sperber et al., 1997; McPhaden, 1999; Seo and Xue, 2005; Hendon et al., 2007); however, others have argued that MJO has little influence on El Niño. Slingo et al. (1999) and Hendon et al. (1999) demonstrated that the correlation between interannual variations of MJO and the sea-surface temperature anomaly (SSTA) of El Niño is very weak. This debate and uncertainty regarding MJO effects on ENSO continues; therefore, it is necessary to further study the effect of MJO forces on ENSO.

In this study, we explored the effect of stochastic MJO forces on ENSO predictability and attempted to quantitatively compare the impact of the initial error and the MJO uncertainty on the predictability of ENSO. The paper is organized as follows. In section 2, the Zebiak-Cane model and the parameterized form of the stochastic MJO forces is described. An approach called the conditional nonlinear optimal perturbation (CNOP) is introduced in section 3. In section 4, we present the primary results of the numerical experiments and show the effect of MJO uncertainty on the ENSO predictability. Finally, the discussion and conclusions are presented in section 5.

2. ENSO model

2.1 *Zebiak-Cane model*

The Zebiak-Cane model (Zebiak and Cane, 1987) was the first coupled ocean–atmosphere model to simulate the interannual variability of the observed ENSO, and it has been a benchmark in the ENSO community for more than two decades. The Zebiak-Cane model has been widely used in predictability studies and predictions of the ENSO (Zebiak and Cane, 1987; Blumenthal, 1991; Chen et al., 2004; Tang et al., 2008). It is composed of a Gill-type, steady-state, linear atmospheric model and a reduced-gravity oceanic model, which depict the thermodynamic and atmospheric dynamics in the tropical Pacific with oceanic and atmospheric anomalies from the mean climatological state specified from the observations (see Zebiak and Cane, 1987).

The atmospheric dynamics are described by the steady-state, linear, shallow-water equations on an equatorial beta plane. The circulation is forced by a heating anomaly that depends partly on local heating associated with SST anomalies and on low-level moisture convergence (parameterized in terms of the surface wind convergence). Herein, the convergence feedback is a nonlinear process because moisture-related heating is operative only when the total wind field is convergent; this feedback depends not only on the calculated convergence anomaly but also on the specified mean convergence. The important effect of the feedback is to focus the atmospheric response to the SST anomalies into or near the regions of mean convergence, in particular, the Intertropical Convergence Zone and the Southern Pacific Convergence Zone.

The thermodynamics of the model are governed by an evolution equation of the SSTA in the tropical Pacific that includes three-dimensional temperature advection by both the specified mean currents and the calculated anomalous currents. The assumed surface heat flux anomaly is proportional to the local SST anomaly, always acting to adjust the temperature field towards its climatologic mean state, which is specified by observations.

In the model simulations, the atmosphere was previously run with the specified monthly mean SST anomalies to simulate the monthly mean wind anomalies. Then, the ocean component was forced by surface wind-stress anomalies generated from a combination of the surface wind anomalies produced by the atmosphere model and the mean background winds.

2.2 *MJO forcing*

In this study, the effect of stochastic MJO forcing on ENSO predictability was investigated, but the forcing was not considered in a Zebiak-Cane model. Therefore, it was necessary to introduce MJO forcing in a rational fashion into the Zebiak-Cane model. Zebiak (1989) constructed a parameterized form of MJO forcing and investigated the effect of MJO on the ENSO prediction. In this study, we used this rational type of MJO forcing to investigate the effect of MJO forcing on ENSO predictability from the viewpoint of error growth. Zebiak (1989) used the rational MJO forcing method according to the following rules: (1) The low-level wind signal was dominantly zonal in the equatorial region; (2) the 30–60-day period contained most of the power; and (3) the disturbances were energetic in the western Pacific, but weaker (at the sur-

face) in the eastern Pacific. Therefore, the rational MJO forcing method determined by Zebiak (1989) is as follows:

$$\tau_{(x)}(t) = A[R(t) + 2R(t-\Delta t) + R(t-2\Delta t)] \times \cos(\omega_0 t + t_0) \frac{\exp\left[-\left(\frac{y}{10}\right)^2\right]}{\exp\left[-\left(\frac{x-x_0}{10}\right)^2\right]}, \quad (1)$$

where R is a normal random variable with zero mean and unit variance, and t_0 represents a uniform random variable on (0, 2π), and the subscript $_{(x)}$ means the zonal wind-stress. This force was evaluated at time intervals of Δt, which was 10 days for the ZC model. The parameters used for ω_0 and x_0 were $2\pi/40$ d^{-1} and 146°E, respectively, and the amplitude A was set at 0.015 N m^{-2}. The western Pacific region (5°N–5°S, 163.125°E–163.125°W) was forced using the rational MJO forcing method.

Figure 1 shows data corresponding to three 48-month studies of this forcing function. The unit of stress is N m^{-2}, and time is in months. Anomalies as large as the climatological mean stress (∼0.05 N m^{-2}) occurred frequently; the model forcing was possibly stronger than had been previously observed (Madden, 1988; see his Fig. 3). In addition, Fig. 2 shows the SSTA and Ustress (zonal wind stress) versus Niño3 in the model. It shows that El Niño began with an expansion of the warm pool into the eastern Pacific

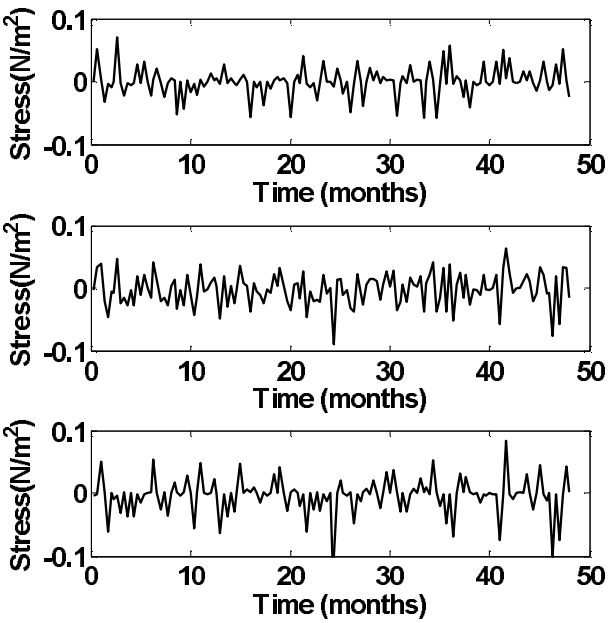

Fig. 1. Three 48-month realizations (units: N m^{-2}) of the stochastic MJO wind-stress forcing.

beginning in May, referred to as May(0) (Fig. 2a). This initial eastward expansion of the warm pool was accompanied by westerly anomalies in the western Pacific (Fig. 2b) in the preceding winter. These results were similar to those shown in Hendon et al. (2007; see his Fig. 8). Therefore, the parameterized form of MJO here was acceptable for our use to investigate the effect of MJO on ENSO predictability.

The MJO forcing parameter had a large degree of uncertainty. What is the evolution of the uncertainty? What is the effect of the MJO forcing uncertainties on ENSO predictability? Between the MJO forcing uncertainty and the initial error, which one has a more important affect on ENSO prediction?

3. Conditional nonlinear optimal perturbations

The CNOP is an initial perturbation that satisfies a given constraint and has the largest nonlinear evolution at the prediction time. The CNOP approach is a natural generalization of the Linear Singular Vector (LSV) approach to a nonlinear regime; it has been used to study the nonlinear dynamics of ENSO predictability (Mu and Duan, 2003; Duan et al., 2004; Duan and Mu, 2006; Mu et al., 2007a, 2007b) and the sensitivity of ocean circulation (Mu et al., 2004). Recently, the CNOP approach has also been used to generate initial perturbations for ensemble prediction (Mu and Jiang, 2008) and to determine the sensitive area in target observations for typhoons (Mu et al., 2009). These studies have shown that CNOP is a useful tool for studying weather and climate predictability. The CNOP approach is briefly reviewed here (Duan et al., 2009a).

The evolution equations for the state vector $\boldsymbol{w}$, which may include surface current, thermocline depth, and SST, among others, can be put into a nonlinear model:

$$\boldsymbol{w}(t) = M_t(\boldsymbol{w}_0), \quad (2)$$

where $\boldsymbol{w}_0$ is an initial value of the model and M_t is the "propagator" that "propagates" the initial value $\boldsymbol{w}_0$ to the future time t. If $\boldsymbol{u}_0$ is an initial perturbation superimposed on a reference state $\boldsymbol{U}(t)$, which is a solution to the nonlinear model and satisfies $\boldsymbol{U}(t) = M_t(\boldsymbol{U}_0)$ ($\boldsymbol{U}_0$ is the initial value of the reference state), the evolution of $\boldsymbol{u}_0$ can be obtained using the following equation:

$$\boldsymbol{u}(t) = M_t(\boldsymbol{U}_0 + \boldsymbol{u}_0) - M_t(\boldsymbol{U}_0). \quad (3)$$

For a chosen norm $\|\cdot\|$, an initial perturbation, $u_{0\delta}$ is called the CNOP, if and only if the following is true:

$$J(\boldsymbol{u}_{0\delta}) = \max_{\|\boldsymbol{u}_0\| \leqslant \delta} \|M_t(\boldsymbol{U}_0 + \boldsymbol{u}_0) - M_t(\boldsymbol{U}_0)\|, \quad (4)$$

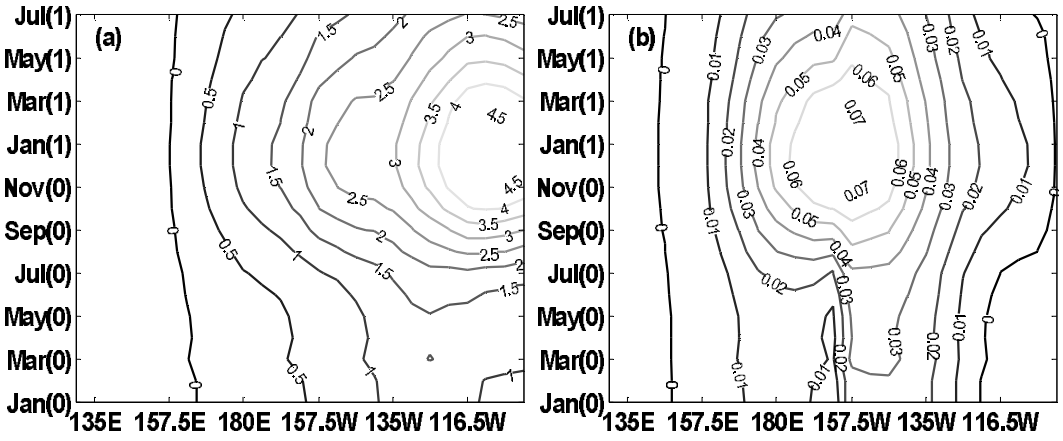

Fig. 2. Monthly regression (contours) of equatorially averaged (a) SST and (b) Ustress onto Niño-3. Contour intervals at (a) 0.5°C and (b) 0.01 N m^{-2}.

where $\|\boldsymbol{u}_0\| \leqslant \delta$ is an initial constraint defined by the norm $\|\cdot\|$, and J is the objective function.

CNOP is the initial perturbation whose nonlinear evolution attains the maximal value of the cost function J at time t. In predictability studies, CNOP represents the initial error that has the worst effect on the prediction result at the optimization time (Mu and Duan, 2003). Therefore, CNOP has been used to identify the initial error that causes the largest prediction error for ENSO events (Xu and Duan, 2008).

To compute CNOP, Eq. (4) must be solved. Eq. (4) is a maximization optimization problem, and no optimization solver is available to calculate it. However, many optimization solvers are readily available to deal with minimization optimization problems. Therefore, we transformed Eq. (4) into a minimization problem by considering the negative of the cost function. Some optimization solvers, such as Spectral Projected Gradient 2 (SPG2: Birgin et al., 2000), Sequential Quadratic Programming, and Limited-memory Broyden–Fletcher–Goldfarb–Shanno, among others, can be used to compute CNOP. The gradient of the modified cost function was necessary in these solvers; furthermore, the adjoint of the corresponding model is usually used to obtain the gradient. With this information on the gradient, running these solvers with initial guesses could aid in the determination of the minimum, modified cost function [i.e., the maxima of the cost function in Eq. (4)] along the descendent direction of the gradient. In a phase space, the point corresponding to the minimum value of the modified cost function is the CNOP defined by Eq. (4). In this study, we used the SPG2 solvers to obtain the CNOP values of the ZC model. To obtain a CNOP, we tried at least 30 initial guesses chosen randomly; if several initial guesses converged to a point in the phase space, this point was considered to be a minimum in the neighborhood. Thus, several such points were obtained. Of these points, the one that made the cost function in Eq. (4) the largest was regarded as the CNOP.

4. Effects of MJO uncertainty on the maximum prediction error for ENSO events

As stated above, MJO is one of the main external forcing events for ENSO. Many studies have used a parameterized form of MJO to investigate the MJO's effect; therefore, there are uncertainties in MJO activities. For example, Zebiak (1989) used a stochastic MJO forcing to study the effect of MJO on ENSO predictions. The stochastic forcing was unpredictable because of its randomicity and was certain to lead to model error. How do model errors evolve, and what is their impact on ENSO predictability? In this section, we will adopt the stochastic rational MJO forcing method to address these questions.

4.1 *Experimental strategy*

Integrating the ZC model for 1000 years, we obtained a time series of SSTA, which provided a great number of El Niño events. These El Niño events tended to have a 4-year period and phase-lock to the end of the calendar year. In numerical experiments, we chose many El Niño events and found that the simulation results depended on the intensities of the El Niño events. Therefore, two groups of El Niño events were used to describe the results: one group consisted of weak events with Niño-3 indices (the SSTA averaged over the Niño-3 region) <2.5°C; the other group included strong events, with Niño-3 indices >2.5°C. Considering that different types of El Niño events exist in nature, we chose four events in each group with initial warming times in January, April, July, and Oc-

tober.

For convenience, we called the Zebiak-Cane model with MJO forcing the ZC–MJO model. We were able to investigate the model errors caused by stochastic MJO forcing on ENSO predictability with the ZC–MJO model. Integrating the Zebiak-Cane–MJO model with the original states of El Niño events as the initial values led to the El Niño events under the influence of model errors produced by stochastic MJO forcing. Comparing the uncertain El Niño events with reference to state events, their difference was in the prediction error caused by stochastic MJO forcing for El Niño events.

To compare the initial error with the model error caused by the stochastic MJO forcing on ENSO predictability, we calculated the initial error, which had the largest impact on the El Niño forecast at the prediction time and could run to a maximum prediction error with a CNOP approach (i.e., CNOP error). The CNOP error in this study was calculated as follows:

We constructed a cost function to measure the evolution of the initial error. The aforementioned CNOP, denoted by $\boldsymbol{u}_{0\delta}$, was obtained by solving the following nonlinear optimization problem:

$$J(\boldsymbol{u}_{0\delta}) = \max_{\|\boldsymbol{u}_0\| \leqslant \delta} \|\boldsymbol{T}'(\tau)\|_2 \ , \tag{5}$$

where $\boldsymbol{u}_0$=$(w_1\boldsymbol{T}'_0, w_2\boldsymbol{h}'_0)$ is a non-dimensional initial error of the SSTA and thermocline depth anomaly superimposed on the initial state of a predetermined reference state El Niño event. Values of w_1=$(2°\mathrm{C})^{-1}$ and $w_2 = (50\,\mathrm{m})^{-1}$ are the characteristic scales of SST and thermocline depth. The constraint condition $\|\boldsymbol{u}_0\| \leqslant \delta$ is defined by a prescribed positive real number δ and the norm

$$\|\boldsymbol{u}_0\| = \sqrt{\sum\nolimits_{i,j} [(w_1\boldsymbol{T}'_{0i,j})^2 + (w_2\boldsymbol{h}'_{0i,j})^2]} \ ,$$

where $\boldsymbol{T}'_{0i,j}$ and $\boldsymbol{h}'_{0i,j}$ represent the dimensional initial error of the SSTA and thermocline depth anomaly at different grid points; position (i, j) is the grid point in the domain of the tropical Pacific with latitude and longitude, respectively, from 129.375°E to 84.375°W by 5.625° and from 19°S to 19°N by 2°. The evolution of the initial error is measured by

$$\|\boldsymbol{T}'(\tau)\|_2 = \sqrt{\sum\nolimits_{i,j} (\boldsymbol{T}'_{i,j}(\tau))^2} \ .$$

The prediction error of SSTA $\boldsymbol{T}'(\tau)$ is represented at time τ and is obtained by subtracting the SSTA of the reference state from the predicted SSTA at prediction time τ.

For each prediction, we calculated the CNOP-type initial errors whose optimization time length was 12 months. Comparing the prediction errors caused by stochastic MJO forcing and CNOP errors and their combined error modes, we investigated the effect of stochastic MJO forcing on ENSO predictability and recognized the main error source affecting ENSO predictability.

Within the context of this study, we used Year(0) to denote the year when El Niño attained a peak value, and we used Year (−1) and Year (1) to signify the year before and after Year (0), respectively. For each El Niño event, we made predictions for 12 months with different starting months. In numerical experiments, the El Niño predictions were made with a starting month of July (−1) [i.e., July in Year (−1)], October (−1), January (0), and April (0).

4.2 *Results*

For convenience, the strong and weak events with initial warming times in January, April, July, and Oc-

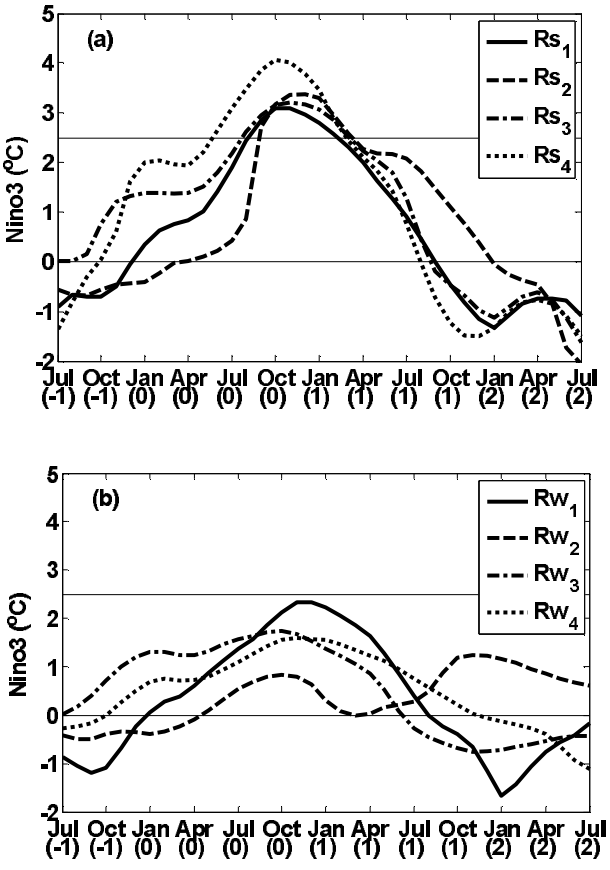

Fig. 3. Two groups of reference-state El Niño events whose initial warming time is January (0) (marked "Rs$_1$" and "Rw$_1$"), April(0) (marked "Rs$_2$" and "Rw$_2$"), July(−1) (marked "Rs$_3$" and "Rw$_3$"), October(−1) (marked "Rs$_4$" and "Rw$_4$"), respectively. (a) The time-dependent Niño-3 indices (units: °C) of four strong El Niño events; and (b) those of four weak El Niño events.

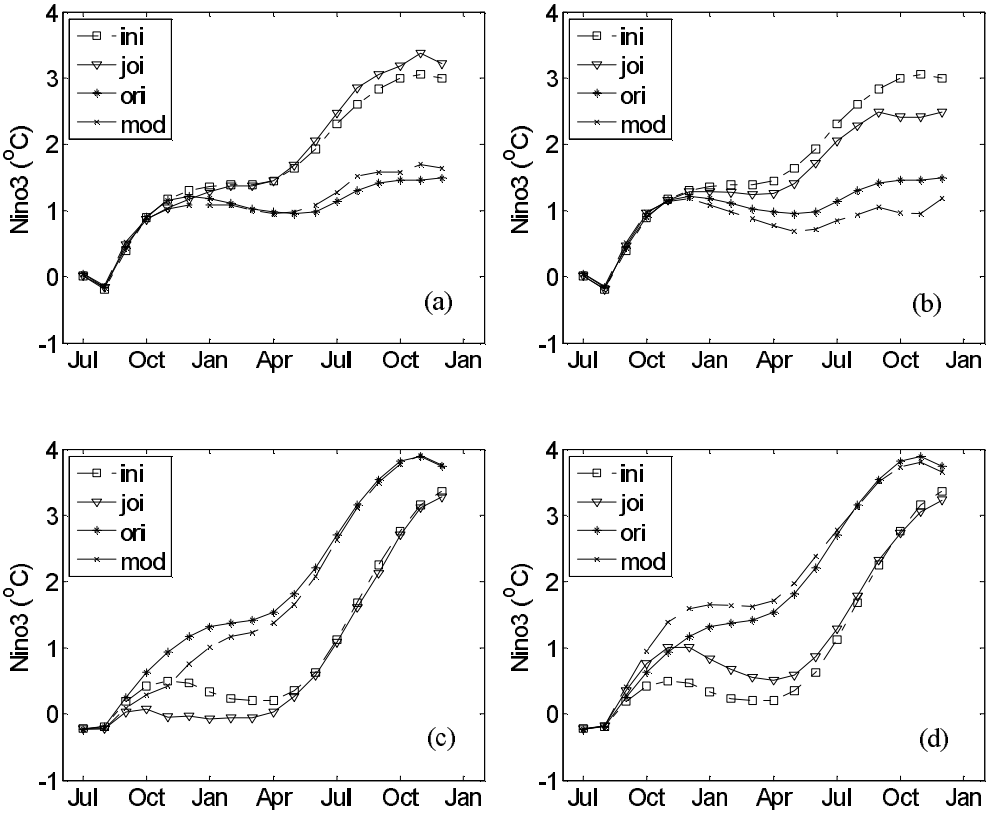

Fig. 4. Predictability experiment (units: °C) of El Niño events initially warming in July(−1). The curves marked "ori" represent the reference state; those marked "mod" represent the results of ZC–MJO model; those marked "ini" represent the results of Zebiak-Cane model; those marked "joi" represent the results of ZC–MJO model with initial errors. Panels (a) and (b) show the predictability experiment of weak El Niño event under the influence of different MJO forcing, respectively. Panels (c) and (d) show the experiment using the strong El Niño event.

tober, were denoted by R_{s_i} and R_{w_i} (i=1, 2, 3, 4). Figure 3 shows the time-dependent Niño-3 indices for these eight El Niño events. The El Niño events with initial warming times in January and April, such as R_{s_1}, R_{s_2}, R_{w_1}, and R_{w_2}, usually reached a peak value in the same year, and those with initial warming times in July and October, such as R_{s_3}, R_{s_4}, R_{w_3}, and R_{w_4}, reached a peak value in the next year.

4.2.1 *Prediction errors caused by stochastic MJO forcing for El Niño events*

First, an investigation into the effect of model errors caused by stochastic MJO forcing on El Niño predictability was conducted. The MJO form described in Eq. (1) of section 2 included the stochastic term. Each numerical realization of the stochastic term was predicted to display different results because of the randomicity; thus, diverse realizations of Eq. (1) exhibited diverse results. Similar to Zebiak (1989), we made nine numerical realizations of stochastic wind stress for each El Niño event to obtain nine different MJO forcings. In the experiments, we imposed each MJO form as an external value into the Zebiak-Cane model and explored the prediction error caused by the stochastic MJO forcing for El Niño. The results demonstrated that some of the stochastic MJO forcing overestimated the El Niño prediction, while others underestimated them. Furthermore, for the weak El Niño events, the stochastic MJO forcing had little effect on the El Niño prediction results in the early stages, while large effects were evident in the latter stages; however, the circumstance was the opposite for the strong El Niño events, i.e., the stochastic MJO had a large effect on the prediction in the early stages, while little effect was evident in the final period. To clarify the results, we displayed the results of the predictability experiment with initial warming time in July for both the weak and strong El Niño events, respectively (Fig. 4). Because the springtime MJO activity is associated with ENSO evolution, we also showed the spring case

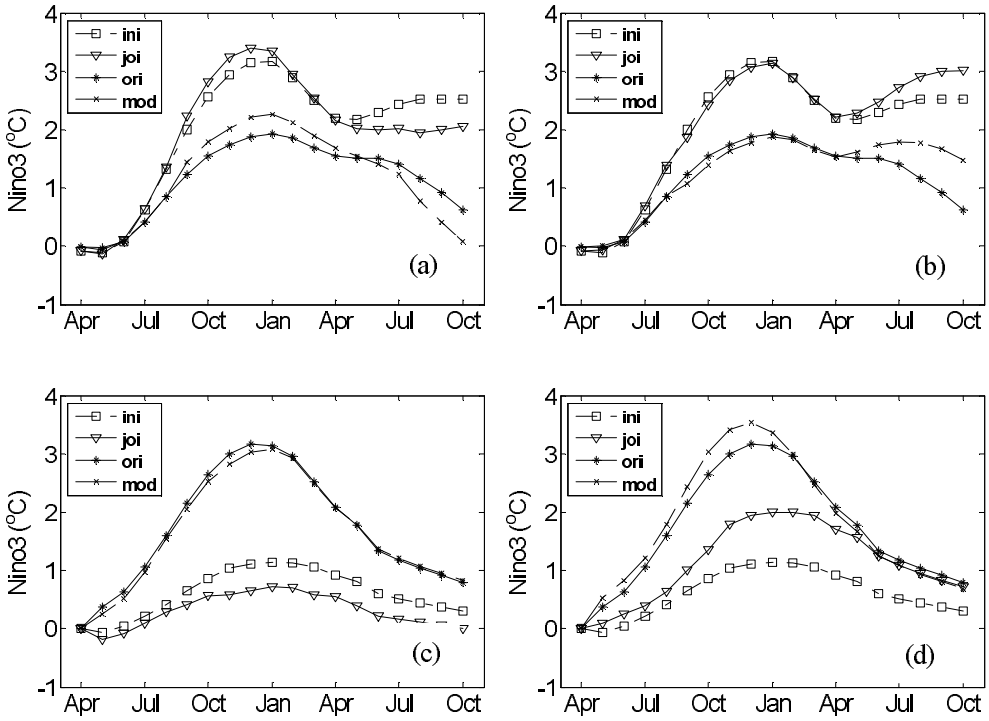

Fig. 5. Predictability experiment (units: °C) of El Niño events initially warming in April(0), which are similar to Fig. 4.

(i.e., the initial warming time in April) in Fig. 5. Clearly, El Niño, under the influence of different MJO forcing values, departed from the reference state differently. For the weak and strong El Niño events with initial warming times in July and April, one numerical MJO realization made the prediction stronger, and the other realizations make the prediction weaker. Moreover, with the initial warming time in July, for weak El Niño events, the MJO forcing had little effect from July in Year (−1) to April in Year (0) (i.e., the early stage), while the effect was large from then on (i.e., the latter stage); however, it was just the opposite for the strong El Niño event. The results were not as obvious with an initial warming time in April, but we could also see that in the last stage, the effect of the MJO forcing had become larger for the weak El Niño events, while the strong El Niño events weakened.

Therefore, we could infer that the impact of the stochastic MJO forcing on the weak El Niño events was higher compared to its impact on the strong events. Of course, this result requires further validation by observational data and concurrent theory.

4.2.2 *Prediction error caused by initial errors*

We calculated the CNOP error for each El Niño prediction whose reference state is displayed in Fig. 3. Piling up the CNOP error on the starting month of each El Niño prediction and then using the perturbed initial value to integrate the Zebiak-Cane model, we obtained the El Niño event affected by the CNOP error (subtracting the reference El Niño event was the maximum prediction error for the reference El Niño). Thus, the CNOP errors damaged the El Niño prediction the most. The maximum prediction error is denoted by $E_{\text{Niño}-3}$, where positive value indicates overprediction of El Niño and negative value indicates underprediction of El Niño.

For the weak El Niño events, the results showed that CNOP errors almost always displayed an overprediction of El Niño; for the strong events, CNOP errors displayed excessively underpredicted values (see Fig. 6).

Figures 4 and 5 show the El Niño events influenced by CNOP errors, which were predicted with an initial field, including CNOP errors. Clearly, the reference El Niño events, which exhibit few differences compared to the results of the ZC–MJO model, were discrepant with the events affected by the initial errors. Thus, compared to the El Niño events impacted by stochastic MJO forcing, the difference between the reference El Niño events and those caused by CNOP errors were much larger between the reference events and those affected by stochastic MJO forcing. The prediction error caused by stochastic MJO error was much smaller than what was produced by the initial error (Fig. 6). Therefore, the main source of error leading to the ENSO

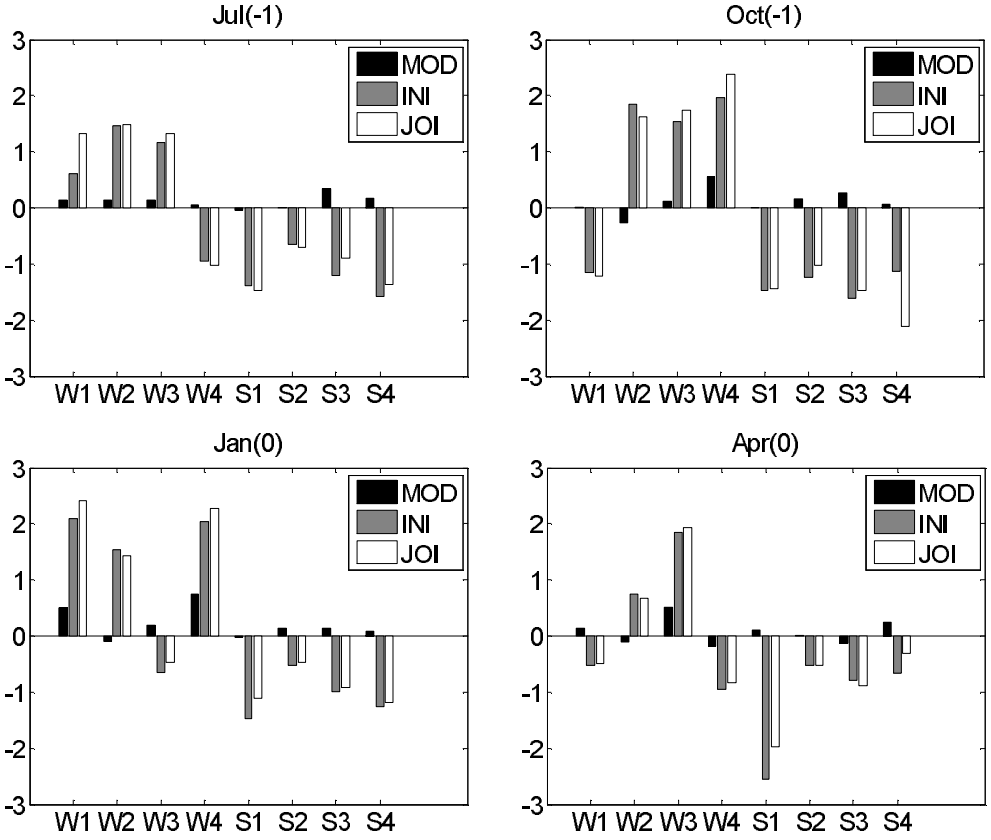

Fig. 6. Prediction errors of Niño-3 indices (units: °C) of the eight El Niño events with starting months of July (−1), October (−1), January(0), and April(0). All the predictions correspond to the same numerical MJO forcing. The symbol "MOD" stands for the prediction errors caused by the stochastic MJO forcing; "INI" indicates those caused by initial errors; "JOI" indicates those resulted from the combined mode of initial errors and model errors.

uncertainty prediction was probably not from model error caused by stochastic MJO forcing, but from the uncertainty of the initial field in the ENSO prediction model. To further demonstrate the problem, we performed another numerical experiment described in the next section.

4.2.3 *The prediction error caused by the combined mode of the initial error and the model error produced by stochastic MJO forcing for El Niño events*

In the actual ENSO prediction, the ENSO model contained both the initial and model error. Therefore, in this section, we further investigated the effect of the combined mode of the initial and model error produced by the stochastic MJO forcing on the ENSO prediction error. Calculating the impact of CNOP error in the initial field of the ZC–MJO model and integrating the model, we attained the El Niño events affected by the joint error mode of the CNOP and model error caused by stochastic MJO forcing. Then, the El Niño events and those affected only by CNOP error were compared. The results demonstrated that the El Niño events affected by the joint error mode were close to those impacted by the initial error (see Figs. 4 and 5); moreover, the Niño-3 index prediction errors that resulted from the initial and joint error mode have little discrepancy (see Fig. 6). In view of the chosen stochastic MJO forcing, which had a similar characteristic and intensity compared to the observation and a smaller prediction error than the initial errors (see also in section 4.2.4), we think that the model error produced by stochastic MJO forcing had little effect on the ENSO uncertainty prediction and that the initial error was probably the primary source of error for the ENSO uncertainty prediction.

Though the impact of the model error caused by the stochastic MJO forcing on the ENSO uncertainty prediction was very small, some small El Niño events affected by the joint error mode were stronger than those impacted by the CNOP error; other events affected by joint error were weaker, but for the strong

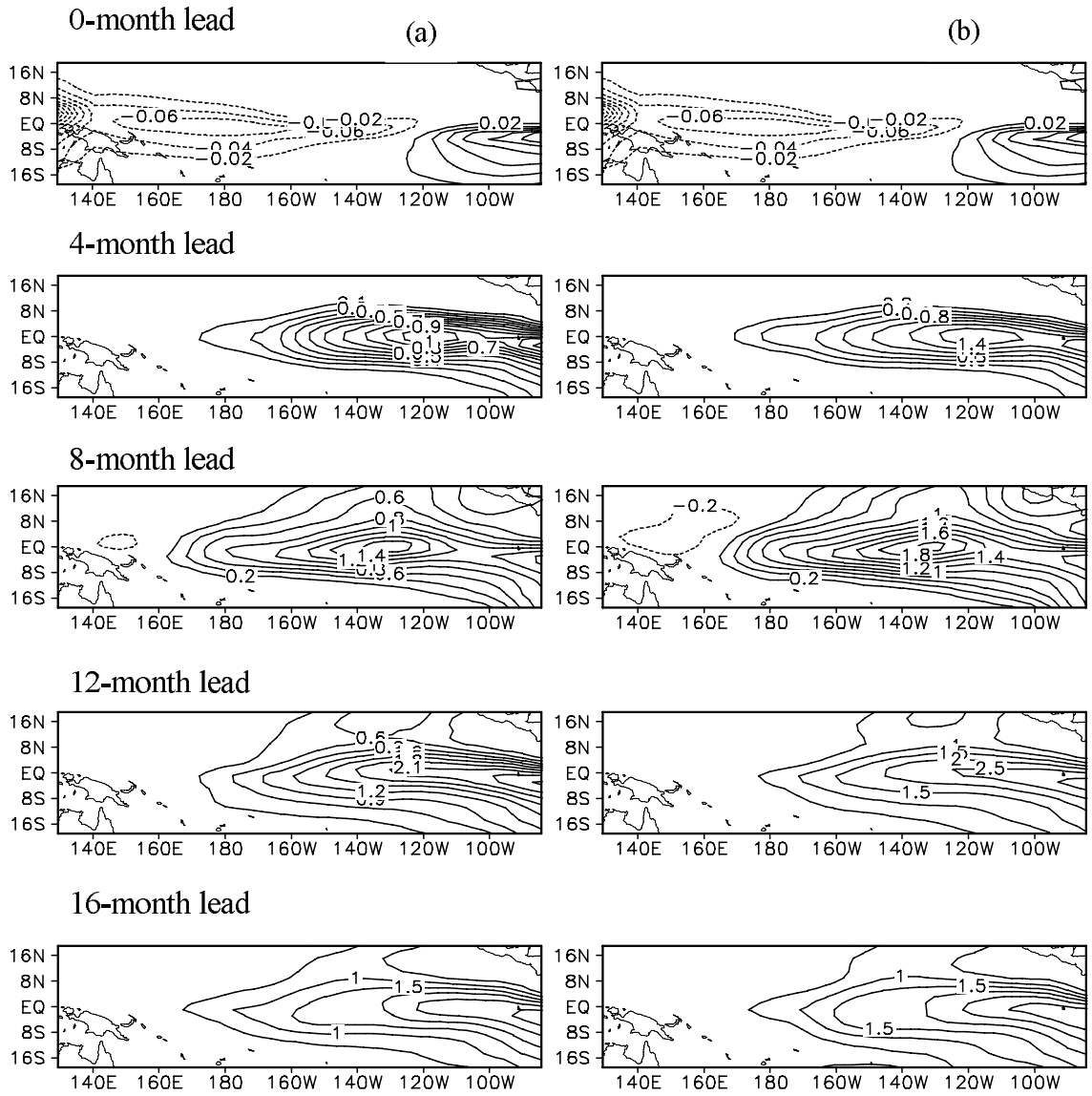

Fig. 7. The SSTA patterns (units: °C) of the evolutions of the composite type-1 CNOP errors with a 0-month lead, a 4-month lead, an 8-month lead, a 12-month lead, and a 16-month lead. (a) The evolution of errors in the Zebiak-Cane model; and (b) the ZC-MJO model, which was the ensemble mean of nine MJO forcings.

El Niño events, the discrepancy was much smaller (see Figs. 4 and 5). The results demonstrated that the stochastic MJO forcing possibly had a large effect on weak El Niño events, while having little effect on strong events. Of course, this result was determined by an empirical approach and needs further validation by observational data and concurrent theory.

4.2.4 *The effect of stochastic MJO forcing on the pattern of initial error*

Studies by Yu et al. (2009) have shown that the CNOP-type initial error can be divided into two types: the SSTA field of the first CNOP-type error has the pattern of positive anomaly in the eastern Pacific and a negative anomaly in the central and western Pacific; the second CNOP-type error has almost the opposite pattern. Furthermore, the two types of errors indicate two mechanisms of error growth in the ENSO prediction: one is the development of initial error that has the same growth behavior of El Niño events; the other is the development of initial error that has the opposite trend of El Niño. We also gained two similar types of CNOP error (see the first picture in Figs. 7 and 8). The errors of SSTA in Niño-3 area were usually less

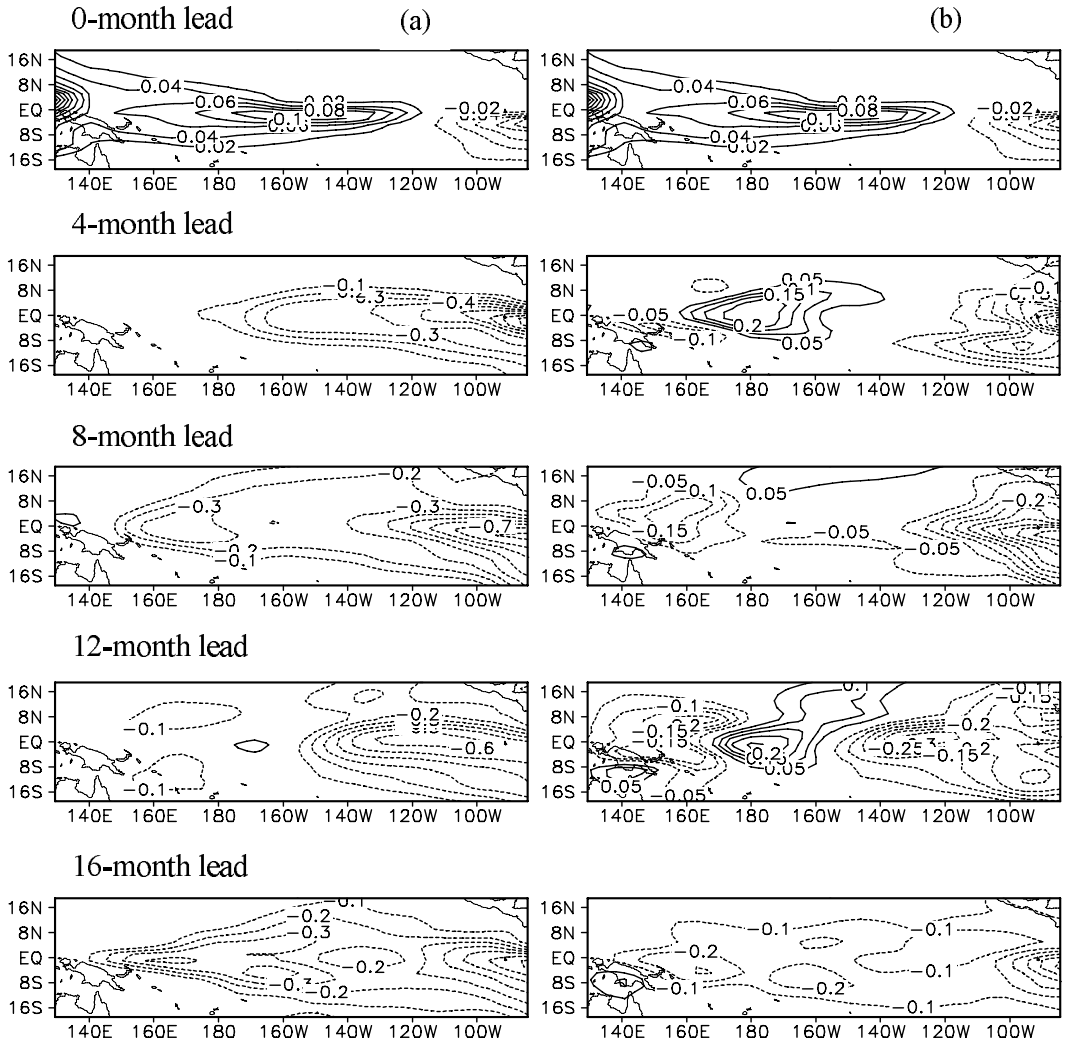

Fig. 8. The SSTA patterns (units: °C) of the evolutions of the composite type-2 CNOP errors which are similar to Fig. 7.

than 0.1°C for the CNOP error, while the observed SST error and the error of analytical SSTA were more than 0.2°C (Kaplan et al., 1998; Reynolds et al., 2002). Hence the initial errors that were larger than CNOP errors were easily visible in the actual ENSO prediction. What is the effect of the stochastic MJO forcing on the evolvement of CNOP error found in this study?

To explore the effect of the model error caused by the stochastic MJO forcing on the evolving CNOP-type initial error, we appended the CNOP error into the initial field of the Zebiak-Cane model and the Zebiak-Cane–MJO model; then, the evolutive spatial pattern of their prediction error of SSTA were compared. Figures 7 and 8 show the evolvement of two types of CNOP errors in the two models. The evolution of CNOP error in the Zebiak-Cane model is on the left, and the ZC–MJO model is on the right. The pattern of two types of CNOP errors evolved into something similar to El Niño and La Niña, while the evolutive trend was analogous to the ZC–MJO model. The distinction indicated that the effect of MJO usually increased the SSTA in the central and eastern Pacific, i.e., SST warming. In fact, previously mentioned studies have pointed out that MJO and the related western wind burst can give rise to remote compelling to the eastern equatorial Pacific by westerly wind anomalies (Hendon et al., 1998; McPhaden and Zhang, 2002) that could bring a sinking Kelvin wave, which can propagate to the central and eastern Pacific, along the thermocline; this can also lead to the phenomenon of raising the sea level along the western coast of South America after the western wind burst ∼6–7 weeks later. Concurrently, the abnormal surface current can lead to an eastern shift of the east-

ern boundary in the warm pool in the western Pacific along the equator. Both of the zonal currents and the thermocline submergence create the SST increase in the central and eastern Pacific. However, the effect of the MJO was much smaller than the evolution of the initial error. Clearly, although the results in the left and right in Figs. 7 and 8 exhibit some differences in numerical value, their spatial patterns had little discrepancy. This further verifies that the initial error is probably the main error source resulting in the uncertainty of ENSO prediction.

5. Summary and discussion

In this study, the effect of model error caused by stochastic MJO forcing on the ENSO predictability was studied and compared to the prediction error that resulted from the CNOP-type initial error using the Zebiak-Cane model and a parameterized form of the MJO forcing. The main results were as follows. For the weak El Niño events, the stochastic MJO forcing had little effect on the prediction results in the initial stages, while large effects were evident in the terminal stages; for the strong El Niño events, the opposite effect was observed. The impact of the stochastic MJO forcing on weak El Niño events may have been higher than on the strong events. In terms of the spatial pattern, the MJO usually increased the SSTA in the central and eastern Pacific. Clearly, the stochastic MJO forcing had an effect on ENSO predictability, but it was less than that of the initial errors. Therefore, the initial error was probably the primary error source that led to the uncertainty of the ENSO prediction.

The results suggest that more attention should be given to the precision of the initial field in ENSO prediction. We noticed that the area of the CNOP-type initial error was concentrated and that it had obvious characteristics of locality. This CNOP error indicated the sensitive area of the ENSO prediction. If we increased the observation in the sensitive area and reduced the opportunity of the CNOP error in an actual ENSO forecast, the forecast skill would possibly improve enormously. Moreover, the dependency of the ENSO predictability on the initial error emphasized in these results provided a theoretical base for the adaptive data assimilation of the ENSO forecast.

Zebiak (1989) posed the following question: "Is there any feature that is symptomatic of an uncertain future evolution, beyond our imperfect knowledge of the state of the system at any given time?" The results of this study have provided some answers to this question: The initial field of the coupled ENSO system determined the future predictability in great part, and the precursor leading to a maximum uncertain future evolution had the pattern of CNOP error.

Further results, discussions, and investigations are needed to complete this study and to settle this debate. For example, if the actual observational MJO data were used, would the results also support those with a parameterized MJO form in this study? In addition, the Zebiak-Cane model used in this paper to study the effect of the MJO on the ENSO predictability was relatively simple, and a more complicated air–sea coupled model is required to further explore the problem. Moreover, it is necessary to investigate whether the results are model dependent. In conclusion, further research is needed to investigate the problems encountered in this paper; the theoretical results of this study may be applied to improve the model and to enhance the ENSO forecast accuracy.

Acknowledgements. The authors thank the two anonymous reviewers for their insightful and detailed comments. This work was jointly sponsored by the Knowledge Innovation Program of the Chinese Academy of Sciences (Grant No. KZCX2-YW-QN203), the National Basic Research Program of China (Grant Nos. 2012CB955202 and 2010CB950402), and the National Natural Science Foundation of China (Grant No. 40821092).

REFERENCES

Birgin, E. G., J. M. Martinez, and M. Raydan, 2000: Nonmonotone spectral projected gradient methods on convex sets. *SIAM Journal on Optimization*, **10**, 1196–1211.

Blumenthal, M. B., 1991: Predictability of a coupled atmosphere-ocean model. *J. Climate*, **4**, 766–784.

Chen, D., and M. A. Cane, 2007: El Niño prediction and predictability. *J. Comput. Phys.* **227**, 3625–3640.

Chen, D., S. E. Zebiak, and A. J. Busalacchi, 1995: An improved procedure for El Niño forecasting: Implications for predictability. *Science*, **269**, 1699–1702.

Chen, D., M. A. Cane, and A. Kaplan, 2004: Predictability of El Niño over the past 148 years. *Nature*, **428**, 733–736.

Duan, W. S., and M. Mu, 2006: Investigating decadal variability of El Niño–Southern Oscillation asymmetry by conditional nonlinear optimal perturbation. *J. Geophys. Res.*, **111**, C07015, doi: 10.1029/2005JC003458.

Duan, W. S., and R. Zhang, 2010: Is model parameter error related to a significant spring predictability barrier for El Niño events? Results from a theoretical model. *Adv. Atmos. Sci.*, **27**(5), 1003–1013, doi: 10.1007/s00376-009-9166-4.

Duan, W. S., M. Mu, and B. Wang, 2004: Conditional nonlinear optimal perturbation as the optimal precursors for ENSO events. *J. Geophys. Res.*, **109**, D23105.

Duan, W. S., F. Xue, and M. Mu, 2009a: Investigating a

nonlinear characteristic of El Niño events by conditional nonlinear optimal perturbation. *Atmos. Res.*, **94**(1), 10–18.

Duan, W. S., X. C. Liu, K.Y. Zhu, and M. Mu, 2009b: Exploring the initial errors that cause a significant "spring predictability barrier" for El Niño events. *J. Geophys. Res.*, **114**, C04022, doi: 10.1029/2008JC004925.

Hendon, H. H., B. Liebmann, and J. D. Glick, 1998: Oceanic Kelvin waves and the Madden-Julian Oscillation. *J. Atmos. Sci.*, **55**, 88–101.

Hendon, H. H., C. Zhang, and J. D. Glick, 1999: Interannual variation of the Madden-Julian oscillation during Austral Summer. *J. Climate*, **12**, 2538–2550.

Hendon, H. H., C. W. Matthew, and C. Zhang, 2007: Seasonal dependence of the MJO-ENSO relationship. *J. Climate*, **20**, 531–543.

Huang, R. H., 1999: Advance of the studies of the characteristics, cause of formation and prediction study for climate disaster in China. *Chinese Academy of Sciences Bulletin*, **3**, 188–199. (in Chinese)

Kaplan, A., M. Cane, and Y. Kushnir, 1998: Analyses of global sea surface temperature 1856–1991. *J. Geophys. Res.*, **103**, 18567–18589.

Luo, J. J., S. Masson, and S. Behera, 2008: Extended ENSO predictions using a fully coupled ocean-atmosphere model. *J. Climate*, **21**, 84–93.

Madden, R. A., 1988: Large intraseasonal fluctuations in wind stress in the tropics. *J. Geophys. Res.*, **93**, 5333–5340.

McPhaden, M. J., 1999: Equatorial waves and the 1997–98 El Niño. *Geophys. Res. Lett.*, **26**, 2961–2964.

McPhaden, M. J., and D. Zhang, 2002: Slowdown of the meridional overturning circulation in the upper Pacific Ocean. *Nature*, **415**, 603–608.

Moore, A. M, and R. Kleeman, 1996: The dynamics of error growth and predictability in a coupled model of ENSO. *Quart. J. Roy. Meteor. Soc.*, **122**, 1405–1446.

Mu, M., and W. S. Duan, 2003: A new approach to studying ENSO predictability: Conditional nonlinear optimal perturbation. *Chinese Science Bulletin*, **48**, 1045–1047.

Mu, M., and Z. N. Jiang, 2008: A new approach to the generation of initial perturbations for ensemble prediction: Conditional nonlinear optimal perturbation. *Chinese Science Bulletin*, **53**(113), 2062–2068.

Mu, M., L. Sun, and D. A. Henk, 2004: The sensitivity and stability of the ocean's thermocline circulation to finite amplitude freshwater perturbations. *J. Phys. Oceanogr.*, **34**, 2305–2315.

Mu, M., H. Xu, and W. S. Duan, 2007a: A kind of initial errors related to "spring predictability barrier" for El Niño events in Zebiak-Cane model. *Geophys. Res. Lett.*, **34**, L03709, doi: 10.1029/2006GL-27412.

Mu, M., W. S. Duan, and B. Wang, 2007b: Season-dependent dynamics of nonlinear optimal error growth and El Niño-Southern Oscillation predictability in a theoretical model. *J. Geophys. Res.*, **112**, D10113, doi: 10.1029/2005JD006981.

Mu, M., F. Zhou, and H. Wang, 2009: A method to identify the sensitive areas in targeting for tropical cyclone prediction: conditional nonlinear optimal perturbation. *Mon. Wea. Rev.*, **137**, 1623–1639.

Reynolds, R. W., N. A. Rayner, and T. M. Smith, 2002: An improved in-situ and satellite SST analysis for climate. *J. Climate*, **15**, 1609–1625.

Seo, K. H., and Y. Xue, 2005: MJO-related oceanic Kelvin waves and the ENSO cycle: A study with the NCEP global ocean data assimilation system. *Geophys. Res. Lett.*, **32**, L07712, doi: 10.1029/2005GL022511.

Slingo, J. M., D. P. Rowell, and K. R. Sperber, 1999: On the predictability of the interannual behavior of the Madden-Julian oscillation and its relationship with El Niño. *Quart. J. Roy. Meteor. Soc.*, **125**, 583–610.

Sperber, K. R., J. M. Slingo, and P. M. Inness, 1997: On the maintenance and initiation of the intraseasonal oscillation in the NCEP/NCAR reanalysis and in the GLA and UKMO AMIP simulations. *Climate Dyn.*, **13**(11), 769–795.

Tang, Y., Z. Deng, X. Zhou, Y. J. Cheng, and D. Chen, 2008: Interdecadal variation of ENSO predictability in multiple models. *J. Climate*, **21**, 4811–4833.

Xu, H., and W. S. Duan, 2008: What kind of initial errors cause the severest prediction uncertainty of El Niño in Zebiak-Cane model. *Adv. Atmos. Sci.*, **25**, 577–584, doi: 10.1007/s00376-008-0577-4.

Xue, Y., M. A. Cane, and S. E. Zebaik, 1997: Predictability of a coupled model of ENSO using singular vector analysis. Part I: Optimal growth in seasonal background and ENSO cycles. *Mon. Wea. Rev.*, **125**, 2043–2056.

Yu, Y. S., W. S. Duan, H. Xu and M. Mu, 2009: Dynamics of nonlinear error growth and season-dependent predictability of El Niño events in the Zebiak-Cane model. *Quart. J. Roy. Met. Soc.*, **135**, doi: 10.1002/qj.526.

Zebiak, S. E., 1989: On the 30–60 day oscillation and the prediction of El Niño. *J. Climate*, **15**, 1381–1387.

Zebiak, S. E., and M. A. Cane, 1987: A model El Niño-Southern Oscillation. *Mon. Wea. Rev.*, **115**, 2262–2278.

Zhang, R. H., G. Q. Zhou, and J. P. Chao, 2003: On ENSO dynamics and its prediction. *Chinese J. Atmos. Sci.*, **27**, 674–688. (in Chinese)